Cooperative Diffusion of Concentrated Polymer Solutions: A Static and Dynamic Light Scattering Study of Polystyrene in DOP

Taco Nicolai*

Laboratoire de Physico Chemie Macromoleculaire, URA CNRS, Université du Maine, 72017 Le Mans, France

Wyn Brown

Department of Physical Chemistry, University of Uppsala, Box 532, 751 21 Uppsala, Sweden

Received December 8, 1994; Revised Manuscript Received August 28, 1995[⊗]

ABSTRACT: Solutions of polystyrene in DOP were studied as a function of the concentration (0.2−0.9 g/mL) and temperature (−10 to +130 °C) using static and dynamic light scattering. The concentration and temperature dependence of the cooperative diffusion coefficient and the osmotic modulus were determined. The concentration and temperature dependences of the cooperative diffusion coefficient are explained in terms of the concentration and temperature dependence of the osmotic modulus and the solvent mobility. At the concentrations studied, the effect of hydrodynamic interactions is small. Close to the glass transition temperature the solvent mobility is the dominant factor and can be treated in terms of the free volume theory.

Introduction

While the dynamics of polymer solutions have been studied extensively by dynamic light scattering (DLS) at volume fractions below 0.1 and above 0.9,[1] relatively few studies have been done covering the intermediate concentrations.[2,3] There are several reasons for this. One of the main ones is that this concentration regime is exceedingly demanding experimentally. Preparing optically clean samples at these concentrations where the scattering intensity of the polymer is very low has been an almost prohibitive task. However, these experiments are judged to be important, and the provision of experimental data over the entire concentration regime of a binary polymer−solvent system not only provides a basis for testing existing theories but also provides a stimulus for future work. Reference 4 described the behavior of the same system in terms of the segmental dynamics and their interrelationship with the concentration fluctuations. In that study we showed that the concentration fluctuations relax through cooperative diffusion until their relaxation rate closely approaches the relaxation rate for the density fluctuations (the so-called α-relaxation). At this point the relaxation rate of the concentration fluctuations becomes q-independent; i.e., the relaxation rate becomes rate-determined by the mobility of the chain backbone. The relaxation time (τ) of the α-relaxation was shown to be well described by the so-called Vogel−Fulcher−Hesse−Tamman (VFHT) equation:

$$\tau = \tau_0 \exp\left(\frac{B}{T - T_0}\right) \tag{1}$$

where T is the absolute temperature. In the concentration range studied (0.7−0.9 g/mL), as well as for the bulk sample, both B and τ_0 were constant within the experimental error while T_0 decreased with decreasing concentration. Earlier studies of semidilute polymer solutions showed that the relaxation of concentration fluctuations occurs mainly through local swelling and deswelling of the transient network formed by entangled polymer chains (see, e.g., Chapter 6 of ref 1). Part of the concentration fluctuations, however, can only relax through structural relaxation of the transient network. The relaxation time characterizing this process is again q-independent and close to the final relaxation time measured in dynamic mechanical measurements. The relative amplitude of this relaxation increases if the osmotic compressibility of the solution decreases and thus depends strongly on the solvent quality. Of course, if the cooperative diffusion is slower than the slowest structural relaxation, only the diffusional relaxation process is observed.

The present paper complements ref 4 with a study of the cooperative diffusion in the transient network over a wide concentration (0.2−0.9 g/mL) and temperature (−10 to +130 °C) range. The results are compared with two theoretical approaches briefly outlined in the next section. One approach is based on the screening of excluded-volume and hydrodynamic interactions by overlapping chains and has been used successfully in the semidilute regime,[5,6] while the other is a free-volume theory applied to concentrated systems not too far from the glass transition temperature, T_g.[7−9] The concepts underlying these two approaches are fundamentally different, and it is of interest to compare their usefulness to describe the dynamics of polymer solutions over a wide concentration and temperature range. For a proper comparison with theory it is necessary to determine the osmotic compressibility as a function of temperature and concentration, which we have done using static light scattering. These results have been interpreted in terms of a Flory−Huggins-type equation.[10]

Experimental Section

In order to obtain optically pure and homogeneous concentrated solutions it is necessary to polymerize styrene in the presence of solvent directly in the measuring cells. The concentrated polystyrene solutions in chromatographic grade (Merck) dioctyl phthalate (bis(2-ethylhexyl phthalate)) were

[⊗] Abstract published in *Advance ACS Abstracts,* January 1, 1996.

0024-9297/96/2229-1698$12.00/0

prepared from dried and vacuum-distilled styrene as previously described[3] by thermal polymerization of the monomer−solvent mixture at 120 °C for 36 h directly in the measuring cells, which were then sealed under vacuum. The conversion in the thermal polymerization was >97%. The samples were characterized using size exclusion chromatography. The number-average molar mass is between 1×10^5 and 2×10^5 g/mol while the weight-average molar mass is between 2×10^5 and 1×10^6. The polydispersity is not expected to have a large influence on the relaxation of the density and concentration fluctuations as this is molar mass independent for the large molar masses and the high concentrations used in this study. Two experimental observations confirm that the influence of polydispersity is small: (1) the glass transition dynamics at high concentrations and without solvent are in agreement with the expected behavior of high molar mass polystyrene (see ref 4), and (2) both the osmotic modulus and the cooperative diffusion coefficient at lowest concentrations agree well with measurements on monodisperse high molar mass samples (see below).

Static and dynamic light scattering measurements were done using an ALV-5000 multibit, multi-τ full-digital correlator in combination with an Ar ion laser emitting vertically polarized light with a wavelength of 488 nm.

Theory

If the relaxation time (τ) measured in DLS is due to cooperative diffusion, the electric field autocorrelation function is a single-exponential decay with relaxation time $\tau = (D_c q^2)^{-1}$, where D_c is the cooperative diffusion coefficient in the laboratory coordinate system and $q = (4\pi n/\lambda)\sin(\theta/2)$ is the scattering vector with n the refractive index of the solution, λ is the wavelength of the incident light, and θ is the angle of observation.[11] D_c is related to the osmotic modulus, $K_{os} = C(\partial\pi/\partial C)$, and the friction coefficient between the polymers and the solvent, f, in the following way:[11,12]

$$D_c = (1-\varphi)^2 (K_{os}/f) \tag{2}$$

where C is the polymer concentration in weight per volume and φ is the polymer volume fraction. Equation 2 contains a thermodynamic and a frictional part, both of which have been treated in various ways. We will briefly discuss the two approaches referred to in the Introduction.

(I) Above the overlap concentration, C^*, the average position of segments belonging to the same polymer is considered to be only correlated over a distance ξ_s due to screening of excluded-volume interactions by other overlapping polymers. The same excluded-volume interactions will cause K_{os} to increase with increasing concentration. If the excluded-volume interactions are weak, i.e., in poor solvents, mean field theory can be used to calculate the concentration dependence of the osmotic modulus and ξ_s. In θ solvents, $K_{os} \propto C^3$ and $\xi_s \propto C^{-1}$. In good solvents one has to take into account that the polymer coils are swollen at distances smaller than ξ_s. Scaling arguments give $\xi_s \propto C^{-0.75}$ and $K_{os} \propto kT/\xi_s^3 \propto C^{2.25}$, with k the Boltzmann constant and T the absolute temperature. The same relations were obtained by Muthukumar and Edwards,[13,14] who modified the Flory−Huggins equation to take into account the correlation between connected segments. Experimentally these power law dependences are observed up to $C \cong 0.2$ g/L for polystyrene (see, e.g., refs 15−17).

Hydrodynamic interactions are also screened by overlapping chains. The hydrodynamic screening length, ξ_h, is proportional to ξ_s both in good and in θ solvents.[18] Using scaling arguments, the cooperative diffusion coefficient becomes

$$D_c = (1-\varphi)^2 \frac{kT}{6\pi\eta_s R_h^a} \tag{3}$$

where R_h^a is an apparent hydrodynamic radius proportional to ξ_h. Experimentally, R_h^a is found to be proportional to ξ_s up to $C \cong 0.2$ g/mL.[17]

The results given above are no longer valid if ξ_s becomes comparable to the Kuhn length of the polymer chains. At higher concentrations, the detailed structure of the polymers becomes important. For polystyrene ξ_s is smaller than the persistence length ($l_p \cong 1$ nm) at $C > 0.15$ g/mL in good solvents and $C > 0.6$ g/mL in θ solvents. At such concentrations, all hydrodynamic interactions are expected to be screened. In this approach, the mobility of the solvent is assumed to be independent of the polymer concentration. The increase of f in eq 2 with increasing concentration is assumed to be entirely due to hydrodynamic screening.

(II) Making use of the fact that the self-diffusion coefficient of the polymer, D_p, is much smaller than that of the solvent, D_s, Vrentas et al.[7,9] derived an expression for the cooperative diffusion coefficient in terms of D_s. In terms of the terminology used here, D_c becomes

$$D_c = \frac{D_s}{A}\frac{(1-\varphi)M_s V_s}{RTV_p}\left(\frac{\partial\pi}{\partial C}\right) \tag{4}$$

with

$$A = \left(\frac{M_s V_s D_s}{M V_p D_p}\right)_{C\to 0}(1-\varphi)^2 + 3\varphi - 2\varphi^2$$

Here V is the partial specific volume, M_s is the molar mass of the solvent, and R is the gas constant. The indexes p and s indicate polymer and solvent parameters, respectively. The first term of the factor A was chosen to give $D_c = D_p$ for $\varphi \ll 1$. This choice leads to wrong values of D_c in semidilute solutions, where the screening effect of hydrodynamic interactions is important. However, if φ is not very small, this term becomes negligible with respect to the other terms. Equation 4 is experimentally observed to work very well down to low concentrations. The next step is to express D_s in terms of free-volume parameters:

$$D_s = D_\infty \exp\left(-\frac{E}{RT}\right)\exp\left[-\frac{\gamma(\omega_s V_s^* + \omega_p \xi V_p^*)}{V_{FH}}\right] \tag{5}$$

with the hole free volume given by

$$V_{FH} = \omega_s k_s (T - T_{0s}) + \omega_p k_p (T - T_{0p}) \tag{6}$$

Here, ω is the mass fraction, V^* is the specific hole free volume required for a jump of either a solvent or a polymer jumping unit, and ξ is the ratio of the critical molar volume of the solvent jumping unit to that of the polymer jumping unit. T_0 is the temperature where V_{FH} becomes zero. E is the energy per mole that a molecule needs to overcome attractive forces which hold it to its neighbors. The temperature and concentration variation of the energy term is expected to be weak compared to the effect of free volume so that this term can be incorporated in the prefactor D_∞. γ is an overlap factor to account for the fact that the same free volume is

available to more than one jumping unit, and k is a free-volume parameter related to the expansion coefficient. We can rewrite eq 5 in the form of the VHFT equation:

$$D_s = D_\infty \exp\left(-\frac{B}{T - T_0}\right) \tag{7}$$

with

$$T_0 = \frac{k_s\omega_s T_{0s} + k_p\omega_p T_{0p}}{k_s\omega_s + k_p\omega_p} \tag{8}$$

$$B = (\omega_s V_s^* + \omega_p \xi V_p^*)/\left(\omega_s\frac{k_s}{\gamma} + \omega_p\frac{k_p}{\gamma}\right) \tag{9}$$

T_0 is the temperature where the friction coefficient becomes infinite and is about 50 °C below T_g.[19] Alternatively, we can write D_s in terms of an effective local viscosity, η_{eff}, and the hydrodynamic radius of the solvent molecules, R_{hs},:

$$D_s = \frac{kT}{6\pi\eta_{eff}R_{hs}} \tag{10}$$

with

$$\eta_{eff} = \eta_o \exp\left(\frac{B}{T - T_0}\right) \tag{11}$$

R_{hs} is not expected to have a strong temperature or concentration dependence. At very low polymer concentrations, η_{eff} reduces to η_s. Combining eqs 4 and 9 we can express D_c in terms of η_{eff}:

$$D_c = (1 - \varphi)^2\frac{kT}{6\pi\eta_{eff}R_h^a} \tag{12}$$

with

$$R_h^a = R_{hs}\frac{RTV_pA(1 - \varphi)}{(M_sV_s)}\left(\frac{\partial\pi}{\partial C}\right)^{-1} \tag{13}$$

In this approach, hydrodynamic interactions are not considered explicitly, which is reasonable at high concentrations.

Equation 12 can be used over the whole concentration range if we realize that R_h^a contains contributions from both excluded volume and hydrodynamic interactions. In very dilute solutions R_h^a is equal to the hydrodynamic radius while in semidilute solutions R_h^a is proportional to ξ_s. In both cases, $\eta_{eff} = \eta_s$. In concentrated solutions all hydrodynamic interactions are screened so that R_h^a is essentially determined by the osmotic compressibility $R_h^a \propto (\partial\pi/\partial C)^{-1}$. The concentration regime where we can assume $\eta_{eff} = \eta_s$ depends on the temperature. Close to the glass transition temperature, η_{eff} will differ from η_s even at low concentrations.

In both approaches the influence of topological constraints is neglected. Topological constraints give rise to a frequency-dependent elastic modulus. However, at the temperature and concentration range studied here, the elastic modulus is small compared to the osmotic modulus and its effect on D_c can be neglected.

Results and Discussion

Osmotic modulus. The osmotic modulus is related to the measured time-averaged scattered light intensities (I) as[20]

$$K_{os} = \left(\frac{KC}{R}\right)RTC \tag{14}$$

Here R is the gas constant and R is the so-called Rayleigh ratio, which we obtained by using toluene at 20 °C as a standard: $R = [(I - I_0)/I_{tol}]R_{tol}(n_s/n_{tol})^2$. I_0 is the intensity scattered by the pure components which should be a weighted average of pure DOP and pure polystyrene. It is difficult to measure accurately the temperature-dependent scattered light intensity of pure polystyrene. Since the scattered light intensity of pure DOP and pure polystyrene are the same within experimental error, we can take the former as I_0 over the whole concentration range. This correction is in any case only important for the highest concentrations. The constant K in eq 14 is proportional to the refractive index increment ($\partial n/\partial C$): $K = 4\pi^2n^2(\partial n/\partial C)^2/N_A\lambda^4$, where N_A is Avogadro's number. For an accurate determination of the osmotic compressibility from the scattered light intensity, we need to take into account the temperature and concentration dependence of the density and refractive index of the solutions. The densities (ρ) of DOP and polystyrene are 1.05 and 0.975 g/mL, respectively, at 20 °C with $\partial\rho/\partial T$ equal to -7.55×10^{-4} and -6.05×10^{-4} g/mL^{-1} K^{-1} for $T > T_g$.[21] The effect of nonideal mixing can be neglected. In the following, we have used φ(mL/mL) = ω(g/g) = C(20 °C; g/mL) for all concentrations and temperatures, which introduces an uncertainty in these parameters of less than 10%. The refractive indices of DOP and polystyrene are 1.485 and 1.59, respectively, at 20 °C with $\delta n/\delta T$ equal to -4.5×10^{-4} K^{-1} and -4×10^{-4} K^{-1}, respectively.[22] The concentration dependence of the refractive index was measured up to 0.2g/L, giving a refractive index increment of 0.103 mL/g with a negligible temperature variation. No curvature in the concentration dependence of the refractive index is expected as the values at lower concentrations extrapolate linearly to the refractive index of pure polystyrene. For the Rayleigh ratio of toluene at 20 °C we have taken 4.0×10^{-5} cm^{-1}.[23] The lower temperature limit at which the intensities can be measured is the phase separation temperature for the lower concentrations and the glass transition temperature for the higher concentrations. For $C = 0.3$ g/mL, these temperatures are about the same. Close to the glass transition temperature very long measurements are necessary to obtain accurate time-averaged intensities. Up to 75 °C, the intensities could be measured with an experimental error of only a few percent. At higher temperatures the experimental error was larger (±10%), but fortunately, the temperature dependence is no longer strong at these temperatures. In Figure 1 the scattered light intensities are shown as a function of temperature for each concentration. No significant dependence of the intensity on the scattering angle was observed. The values $(I - I_0)/I_{tol}$ of pure polystyrene and $C = 0.9$ g/mL were estimated from measurements at higher temperatures and are 0.7 and 1.5, respectively. The strong increase at low temperatures for $C = 0.2$ and 0.3 g/mL is due to critical fluctuations. The solid lines are fits to the following empirical function: $\log(I) = A + B/(T - T')$, where T' is the critical temperature at which phase separation occurs and the intensity diverges. This equation describes very well the temperature dependence of the intensity and can be used to interpolate between the data, but the temperature range covered for most

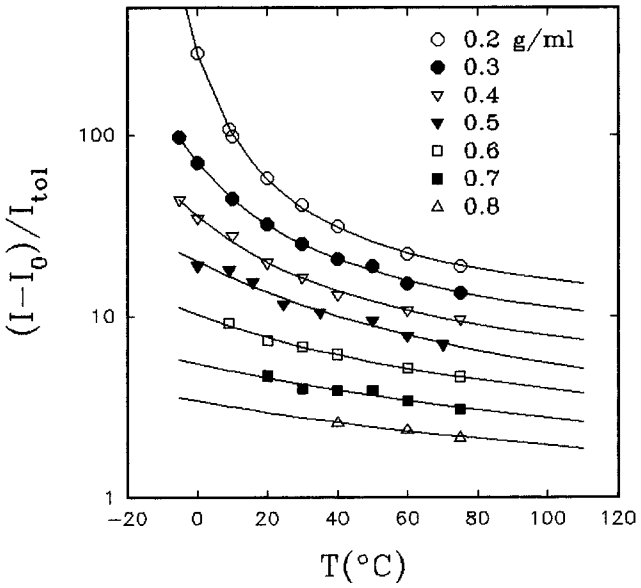

Figure 1. Semilogarithmic representation of the temperature dependence of $[(I - I_0)/I_{tol}]$, where I is the solution intensity, I_0 is that of pure DOP and I_{tol} that of toluene at 20 °C, at various concentrations indicated in the figure. The solid lines represent fits to an empirical function: $\log[(I - I_0)/I_{tol}] = A + B/(T - T')$; see text.

concentrations is too limited to bestow significance to the values of the fit parameters.

We have calculated K_{os} as a function of the polymer volume fraction, φ, for a number of temperatures between 10 and 90 °C using scattered light intensities interpolated from Figure 1 in eq 14 (see Figure 2). Included are measurements on semidilute solutions of high molar mass monodisperse polystyrene ($M_w = 5 \times 10^6$ g/mol) in DOP. The data are compared with the Flory−Huggins equation for the osmotic pressure:[10]

$$\pi = -(RT/v)[\ln(1 - \varphi) + (1 - P^{-1})\varphi + \chi\varphi^2] \qquad (15)$$

where v is the effective molar volume the solvent and P is the number-average polymerization index. χ is an interaction parameter which depends on the temperature, concentration, and the molar mass distribution.[24] To fit the data correctly over the whole concentration range, we need to express χ as a polynomial of the fourth degree

$$\chi = a_1 + a_2\varphi + a_3\varphi^2 + a_4\varphi^3 \qquad (16)$$

Neglecting P^{-1}, we obtain

$$K_{os} = (CRT/v)\left[\frac{\varphi}{(1 - \varphi)} - 2a_1\varphi - 3a_2\varphi^2 - 4a_3\varphi^3 - 5a_4\varphi^4\right] \qquad (17)$$

The results from nonlinear least-squares fits to eq 17 are represented by the solid lines in Figure 2. The optimum values for the fit parameters are given in Table 1. The coefficient a_1 is related to the second virial coefficient: $A_2 = (1 - 2a_1)/(2v)$. At the theta temperature, T_θ, $A_2 = 0$ and $a_1 = 0.5$. Extrapolating the results in Table 1, we obtain $T_\theta \approx 7$ °C, which is much smaller than the value given by Berry,[25] $T_\theta = 22$ °C, which is, as far as we know, the only literature value. We have measured the temperature dependence of A_2 for dilute solutions of monodisperse PS with $M_w = 5 \times 10^6$ g/mol using static light scattering. In Figure 2b, the temperature dependence of A_2 is compared with the values calculated from a_1 in Table 1. T_θ obtained from measurements on very dilute solutions is 12 °C, which is much closer to the value estimated from a_1. Of course, when A_2 is very small the accuracy of the value calculated using a_1 decreases as a_1 approaches 0.5.

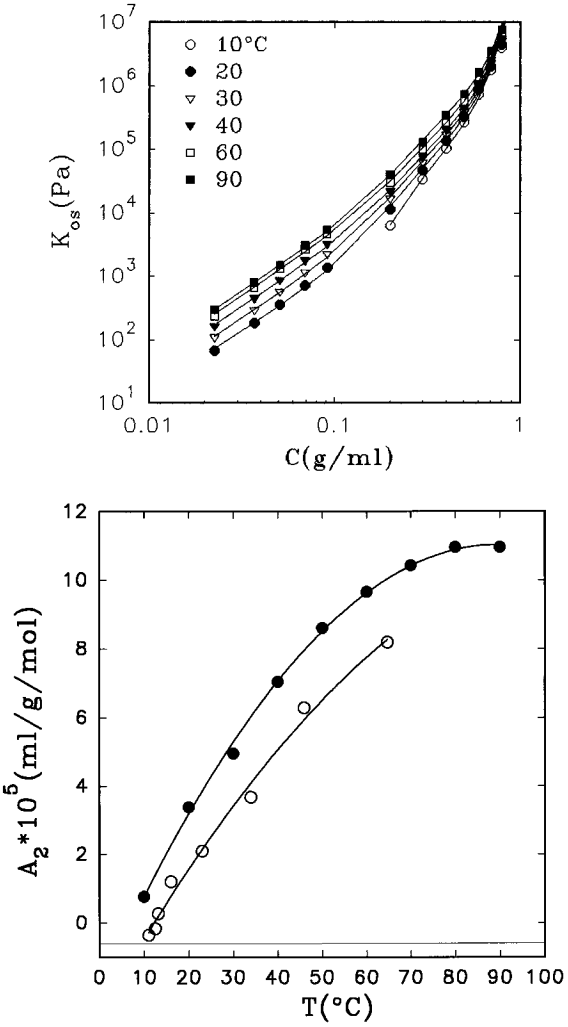

Figure 2. (a, top) Semilogarithmic plot of K_{os} versus the concentration at various temperatures as indicated in the figure. The solid lines represent fits to eq 15. (b, bottom) Comparison of the temperature dependence of the second virial coefficient measured for dilute solutions (open circles) with that of the values calculated from a_1 (filled points) given in Table 1. The solid lines are guides to the eye.

Table 1. Values of the Fit Parameters Obtained from Nonlinear Least-Squares Fits of K_{os} to Eq 17

T (°C)	a_1	a_2	a_3	a_4
10	0.497	0.406	−0.309	0.855
20	0.487	0.398	−0.300	0.844
30	0.481	0.392	−0.333	0.871
40	0.473	0.404	−0.379	0.896
50	0.467	0.414	−0.445	0.944
60	0.463	0.403	−0.428	0.921
70	0.460	0.407	−0.473	0.954
80	0.458	0.426	−0.567	1.026
90	0.458	0.427	−0.610	1.062

Cooperative Diffusion. Relaxation times characterizing the concentration fluctuations were derived from the measured intensity autocorrelation functions by taking the maximum of the relaxation time distribution calculated by inverse Laplace transform analysis as explained in ref 4. The results obtained at a fixed scattering angle (90°) are shown in Figure 3. The dotted

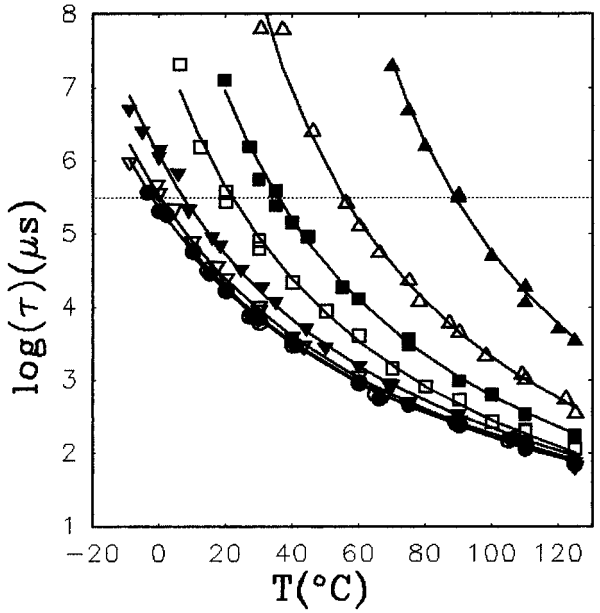

Figure 3. Semilogarithmic representation of the relaxation times measured at $\theta = 90°$ versus temperature for various concentrations. The symbols are the same as in Figure 1 and $C = 0.9$ g/mL is represented by ▲. The solid lines are guides to the eye. The dotted line separates approximately the slower q-independent from the faster q^2-dependent relaxation times.

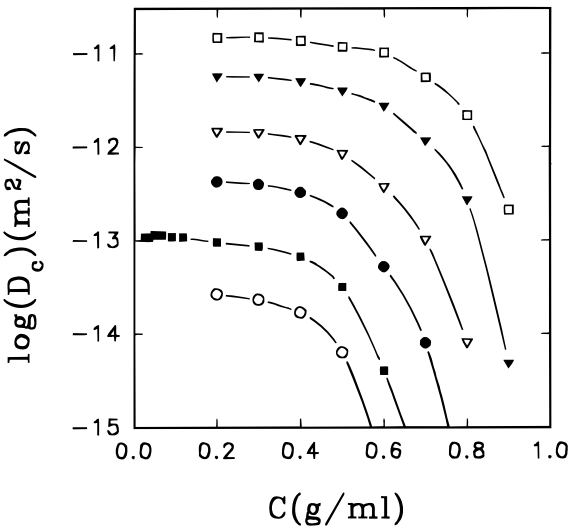

Figure 4. Semilogarithmic plot of the cooperative diffusion coefficient versus the concentration at 10 (○), 22 (■), 40 (●), 60 (▽), 90 (▼), and 120 °C (□).

line indicates approximately the upper limit where the relaxation times are still q^2-dependent at $\theta = 90°$. At higher temperatures, the concentration fluctuations relax through cooperative diffusion while at lower temperature they are strongly coupled to density fluctuations.[4]

The cooperative diffusion coefficient in the laboratory coordinate system is shown in Figure 4 as a function of the concentration for a number of temperatures. Values of D_c measured at 22 °C on lower concentrations of monodisperse high molar mass polystyrene in DOP taken from ref 26 are included for comparison. As mentioned above, the good agreement between these earlier measurements and the present results show that for the concentrations studied here the cooperative diffusion coefficient is molar mass independent and not significantly influenced by polydispersity. D_c decreases very strongly above a certain concentration which

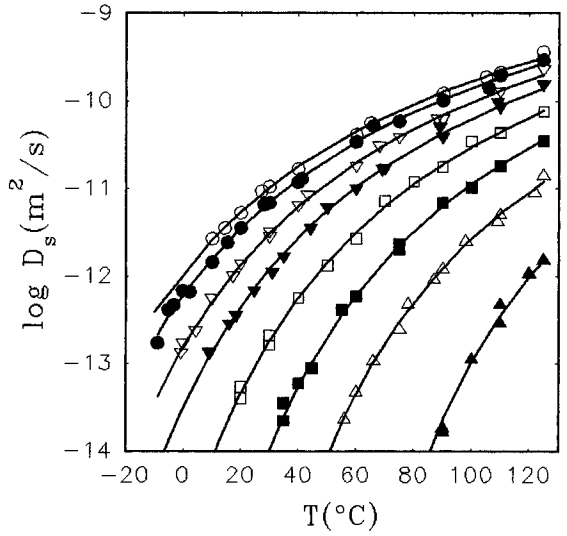

Figure 5. Semilogarithmic representation of the solvent self-diffusion coefficient versus temperature for various concentrations. The symbols are the same as in Figures 1 and 3. The solid lines are guides to the eye.

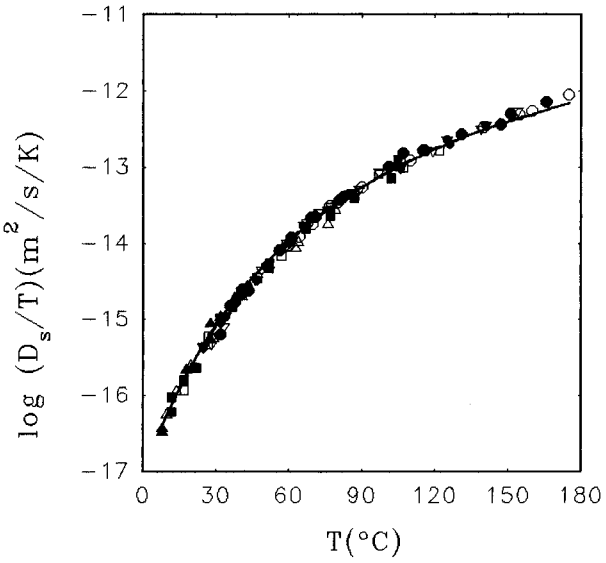

Figure 6. Master curve obtained by temperature−concentration shifts of D_s/T with reference concentration 0.6 g/L. The symbols are the same as in Figures 1 and 3. The solid line represents eq 7 with $B = 1236$, $T_0 = 197$K, and $D_\infty/T = 1.0 \times 10^{-10}$ m^2 s^{-1} K^{-1}.

depends on the temperature. The decrease is due to the reduced solvent mobility when the system approaches the glass transition temperature.

Self-diffusion coefficients of the solvent were calculated using eq 4 and neglecting the first term in A, which is very small at higher concentrations. Values of D_s at each concentration are plotted in Figure 5 as a function of the temperature. Nonlinear least-squares fits to eq 7 gave B between 1080 and 1450 and $D_\infty/T = (1.0 \pm 0.05) \times 10^{-10}$ m^2 s^{-1} K^{-1}. The variation in B is not related to the concentration but reflects the experimental noise and the limited temperature range. In fact, within the scatter of the data, a master curve can be constructed by simple temperature shifts of D_s/T; see Figure 6. The solid line through the master curve with reference concentration 0.6 g/mL represents a fit to eq 7 using $B = 1236$, which gives $T_0 = 197$ K and $D_\infty/T = 1.0 \times 10^{-10}$ m^2 s^{-1} K^{-1}. This value of B was chosen because the temperature dependence of the viscosity of

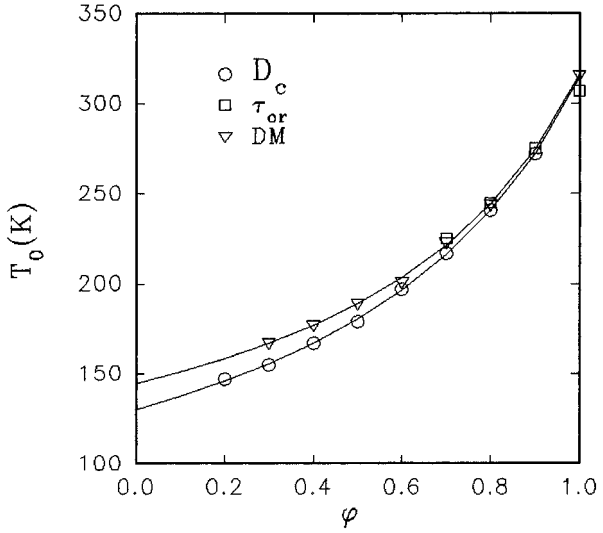

Figure 7. Concentration dependence of the parameter T_0 in the VHFT equation, which characterizes the temperature dependence of D_c (○), density fluctuations (□) (see ref 4), and the shear modulus (▽) (see ref 27). The solid lines represent fits to eq 8.

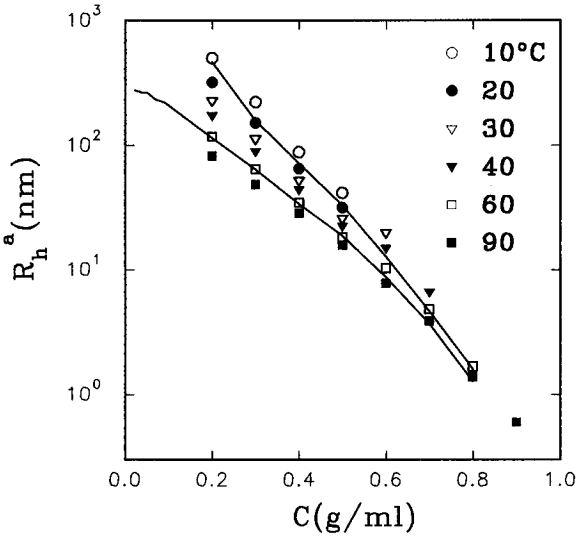

Figure 8. Concentration dependence of R_h^a calculated from D_c using eq 12 at a number of temperatures indicated in the figure. The solid lines represent calculations of R_h^a using eq 13 and experimental values of the osmotic compressibility at 10 and 90 °C.

pure DOP is given by[27]

$$\eta_s = 1.24 \times 10^{-5} \exp\left(\frac{1236}{T - 152.2}\right) \text{Pa·s} \qquad (18)$$

Utilizing $D_\infty/T = 1.0 \times 10^{-10}$ m^2 s^{-1} K^{-1} and $\eta_o = 1.24 \times 10^{-5}$ Pa·s in eqs 7, 10, and 11, we obtain 5.9 Å for the effective hydrodynamic radius of DOP, where it is assumed that the energy term in D_∞ can be neglected. Values of T_0 at other concentrations were calculated from the ΔT values used to construct the master curve and are shown in Figure 7. For comparison we have included T_0 values obtained from the temperature dependence of the α-relaxation measured by DLS.[4] Recently, we measured the temperature dependence of the shear modulus of the same solutions.[28] Master curves of the loss and storage moduli could be obtained from a temperature-frequency superposition. The temperature dependence of the shift parameter is well described by the VHFT equation. T_0 values obtained in this way are also included in Figure 7. At higher concentrations T_0 is the same, which confirms the general belief that the temperature dependence of the friction felt by the solvent molecules is the same as the friction felt by the polymer segments.[19] At lower concentrations T_0 obtained from the diffusion coefficient is somewhat lower. Several reasons could be given to explain the difference at lower concentrations, e.g., a wrong estimate of D_s from D_c or the influence of the energy term in D_∞. It is however, difficult to draw definite conclusions based on the relatively small difference as the measurements on the lower concentrations are done far above T_g where the temperature dependence is rather weak. Direct comparison with T_g values is difficult since differential calorimetric scanning measurements show very broad glass transitions for most concentrations, indicative of inhomogeneities on a local scale. This is most likely due to the fact that T_g is far below the θ temperature for most concentrations. The light scattering measurements are all above or close to the θ temperature, so that possible inhomogeneities do not play a significant role in these measurements. The solid line through the data obtained from the diffusion coefficient represents a nonlinear least-squares fit to eq 8 with $k_p/k_s = 2.7 \pm 0.1$, $T_{0s} = 130 \pm 2$ K, and $T_{0p} = 314 \pm 2$ K.

On the basis of these results, we can calculate the effective viscosity as

$$\eta_{\text{eff}} = 5.0 \times 10^{-12} \exp\left(\frac{1236}{T - T_0}\right) \text{Pa·s} \qquad (19)$$

with $T_o = (351 - 37C)/(2.7 - 1.7C)$ K. Utilizing this expression for η_{eff} in eq 12 we can determine R_h^a from the measured values of D_c; see Figure 8. Alternatively, R_h^a can be calculated according to eq 13 using the experimental values of $\partial\pi/\partial C$. The results at 10 and 90 °C are shown as solid lines in Figure 8. The agreement is very good considering the experimental error. It is clear that at the higher concentrations studied here the effect of hydrodynamic interactions are unimportant and the concentration dependence of R_h^a is mainly due to the concentration dependence of the osmotic compressibility.

Summary

The relaxation time of concentration fluctuations is q^2-dependent at high temperatures and q-independent at low temperatures. The temperature at which the q-dependence changes for a given range of q increases with increasing concentration. In ref 4 it was shown for $C \geq 0.7$ g/mL that the q-independent relaxation time is close to the local segmental relaxation time of the polymer backbone (α-relaxation). It was concluded that the local segmental relaxation is the limiting step for the relaxation of the concentration fluctuations. The temperature dependence of the relaxation time of the concentration fluctuations is very similar over the whole concentration range investigated ($0.2 \leq C \leq 1$ g/mL) apart from a systematic shift to lower temperatures as the concentration is decreased.

The cooperative diffusion coefficient is strongly temperature and concentration dependent. The concentration dependence at fixed temperature cannot be explained solely in terms of a variation of the osmotic compressibility and the hydrodynamic screening length. One has to take into account the reduction of the solvent

mobility due to the presence of polymer chains. A consistent description of the concentration dependence of D_c at fixed temperature is be obtained if one replaces the solvent viscosity by an effective viscosity which diverges at T_g of the solution and takes into account the influence of polymer chains on the solvent mobility.

Acknowledgment. W. B. acknowledges the support of the Swedish Natural Science Research Council (NFR).

References and Notes

(1) For example: *Dynamic Light Scattering*; Brown, W., Ed.; Clarendon Press: Oxford, U.K., 1993.
(2) Koch, T.; Strobl, G.; Stuhn, B. *Macromolecules* **1992**, *25*, 6255.
(3) Brown, W.; Johnsen, R. M.; Konak, C.; Dvoranek, L. *J. Chem. Phys.* **1991**, *95*, 8568.
(4) Brown, W.; Nicolai, T. *Macromolecules* **1994**, *27*, 2470.
(5) Doi, M.; Edwards, S. F. *The Theory of Polymer Dynamics*; Clarendon Press: Oxford, England, 1986.
(6) de Gennes, P.-G. *Scaling Concepts in Polymer Physics*; Cornell University Press: London, 1979.
(7) Vrentas, J. S.; Duda, J. L. *J. Polym. Sci.* **1977**, *15*, 403.
(8) Vrentas, J. S.; Vrentas, C. M. *Macromolecules* **1993**, *26*, 1277.
(9) Vrentas, J. S.; Vrentas, C. M. *Macromolecules* **1993**, *26*, 6129.
(10) Flory, P. J. *Principles of Polymer Chemistry*; Cornell University Press: London, 1953.
(11) Berne, B.; Pecora, R. *Dynamic light scattering*; Wiley: New York, 1976.
(12) Vink, H. J. *J. Chem. Soc., Faraday Trans.* **1985**, *81*, 1725.
(13) Muthukumar, M.; Edwards, S. F. *J. Chem. Phys.* **1982**, *76*, 2720.
(14) Muthukumar, M. *J. Chem. Phys.* **1986**, *85*, 4722.
(15) Stepanek, P.; Perzynski, R.; Delsanti, M.; Adam, M. *Macromolecules* **1984**, *17*, 2340. Nicolai, T.; Brown, W. *Macromolecules* **1990**, *23*, 3150.
(16) Amirzadeh, J.; McDonell, M. E. *Macromolecules* **1982**, *15*, 927. Noda, I.; Kato, N.; Kitano, T.; Nagasawa, M. *Macromolecules* **1981**, *14*, 668.
(17) Brown, W.; Nicolai, T. *Colloid Polym. Sci.* **1990**, *268*, 977.
(18) Muthukumar, M.; Edwards, S. F. *Polymer* **1982**, *23*, 345.
(19) Ferry, J. D. *Viscoelastic Properties of Polymers*, 2nd ed.; Wiley: New York, 1970.
(20) Yamakawa, H. *Modern Theory of Polymer Solutions*; Harper & Row: New York, 1971.
(21) Perry, E. S.; Fuguitt, R. E. *Ind. Eng. Chem.* **1947**, *39*, 782 (DOP). *Polymer Handbook*, 2nd ed.; Brandup, J., Immergut, E. H., Eds.; Wiley: New York, 1975 (polystyrene).
(22) Reed, M. C., Connor. *Ind. Eng. Chem.* **1948**, *40*, 1414 (DOP). *Polymer Handbook*, 2nd ed.; Brandup, J., Immergut, E. H., Eds.; Wiley: New York, 1975 (polystyrene).
(23) Bender, T. M.; Lewis, R. J.; Pecora, R. *Macromolecules* **1986**, *19*, 244.
(24) Fujita, H. *Polymer Solutions*; Elsevier: Amsterdam, 1990.
(25) Berry, G. C. *J. Chem. Phys.* **1966**, *44*, 4553.
(26) Nicolai, T.; Brown, W.; Hvidt, S.; Heller, K. *Macromolecules* **1990**, *23*, 5088.
(27) Floudas, G.; Higgins, J. S.; Fytas, G. *J. Chem. Phys.* **1992**, *96*, 7672.
(28) Nicolai, T.; Brown, W.; Pakula, T., unpublished results.

MA946430P